THE ASTROPHYSICAL JOURNAL, 252:214–229, 1982 January 1

ULTRAVIOLET OBSERVATIONS OF STELLAR CHROMOSPHERIC ACTIVITY

L. HARTMANN,[1] A. K. DUPREE,[1] AND J. C. RAYMOND[1]
Harvard-Smithsonian Center for Astrophysics
Received 1981 February 9; accepted 1981 July 21

ABSTRACT

A survey of chromospheric and transition region (TR) line emission in late-type stars obtained with the *IUE* satellite is presented. We find a wide variation in TR emission (ions formed near $T = 10^5$ K) at a given position in the H-R diagram, in contradiction with theories incorporating only acoustic energy generation and deposition. The behavior of the Hyades giants suggests that age does not uniquely determine emission levels. Our data are consistent with the picture advanced by many others that rapid rotation appears to result in enhanced fluxes. Emission in TR lines is correlated with chromospheric emission; the range in observed surface fluxes from different stars increases with increasing temperature of line formation.

Although emission measures of high temperature gas generally decline with decreasing stellar gravity, it is not possible to define a sharp division in the H-R diagram between stars with TR emitting regions and those without, for several reasons: (1) The sensitivity limit of *IUE* appears to have prevented C IV detections for at least two stars with measured X-ray fluxes. (2) The wide range of TR fluxes at a given point in the H-R diagram introduces selection effects. (3) Stars with C IV upper limits also tend to have low chromospheric emission, so that the relative emission measure distribution cannot be shown to be dropping very sharply with increasing temperature. (4) Stars may have both cool winds and high temperature (10^5 K) line emission.

The temperature structures of the envelopes of late-type stars are also investigated. Very active dwarf stars have emission measure distributions as a function of temperature which are similar to solar active regions. The large N V/C IV ratios typical of hybrid stars may indicate relatively low coronal temperatures. We find that ratios of X-ray and TR emission are roughly compatible with simple loop models. The He II λ1640 fluxes appear to be related to coronal emission and also may be used to investigate the emission measure distributions as a function of temperature.

Subject headings: stars: chromospheres — stars: coronae — stars: late-type — ultraviolet: spectra

I. INTRODUCTION

It has been known for many years that most stars later than about mid-F possess chromospheres (cf. Wilson 1966). It was also suggested from ground-based observations that while late-type giants and supergiants exhibit chromospheric activity, their extended atmospheres are much cooler than the solar wind and corona. Distant circumstellar shells were discovered in lines of low-excitation species (Deutsch 1956, 1960), and there were also arguments which suggested that temperatures $\gtrsim 1 \times 10^5$ K are not attained in the outer atmosphere of the M supergiant α Ori (Weymann 1962). Mullan (1978) predicted that stars more luminous than a certain limit in the H-R diagram would not have coronae; however, the theoretical basis of this argument is questionable (Holzer 1980).

A clear knowledge of the regions of the H-R diagram in which hot ($T \gtrsim 1 \times 10^5$ K) outer atmospheres occur ultimately rests on observations from space, which can detect ultraviolet and X-ray emission. While stellar chromospheric emission in the range 1000–2000 Å was initially observed with the *Copernicus* satellite (Dupree 1975) and by rocket (Vitz *et al.* 1976), the advent of the International Ultraviolet Explorer (IUE) satellite has made it possible to sample chromospheric and transition-region line emission in a fair number of late-type stars (Linsky *et al.* 1978; Brown, Jordan, and Wilson 1979; Dupree *et al.* 1979; Linsky and Haisch 1979; Dupree and Hartmann 1980; Ayres, Marstad, and Linsky 1981). Similarly, while rocket observations first detected X-rays from "normal" late-type stars (Catura, Acton, and Johnson 1975; Topka *et al.* 1979), the *HEAO 2* satellite (*Einstein*) has now made it possible to survey X-ray emission from such stars through the H-R diagram (Vaiana *et al.* 1981).

The initial surveys in the ultraviolet and in the X-ray spectral regions of late-type stars (Linsky and Haisch 1979; Vaiana *et al.* 1981) generally confirmed the picture presented above, that high gravity stars have high temperature ($T \gtrsim 1 \times 10^5$ K) outer atmospheres; low gravity stars show no evidence for gas at temperatures in excess of 2×10^4 K. The exact division between stars with and without hot outer atmospheres is a subject of some debate (Linsky and Haisch 1979; Dupree and Hartmann 1980; Hartmann, Dupree, and Raymond 1980). The detection of hot gas depends not only on stellar properties but on observational constraints as well, which must be con-

[1] Guest Investigator, *International Ultraviolet Explorer* Satellite.

sidered in order to determine the extent of coronal formation in the H-R diagram. Furthermore, the relative distribution of emission measure as a function of temperature must be considered as well in any attempt to interpret the observations in physical terms.

In this paper we present a survey of stellar emission line fluxes detected with *IUE* in the wavelength region 1175–1950 Å, obtained in the low dispersion mode, as well as Mg II fluxes (λ2800) measured at high dispersion. We have estimated the uncertainty in the flux measurements for detected lines and have carefully constructed upper limits to the fluxes of undetected high temperature lines. From these data, we are able to infer the temperature structure of the outer atmospheres of cool stars and to investigate the variation of emission line strength and the general presence of hot outer atmospheric gas throughout the H-R diagram.

II. OBSERVATIONS

The emission line fluxes reported here in the short wavelength (SWP) (1150–1950 Å) region were obtained in the low resolution mode ($\sim$ 6 Å resolution) of the *IUE* satellite in 1978, 1979, and 1980 (Boggess *et al.* 1978). These spectra, originally processed with the incorrect Intensity Transfer Function, were corrected with the three agency fourth file method (cf. Cassatella *et al.* 1980). The May 1980 calibration was used (Bohlin and Holm 1980). Sample SWP spectra of giant and dwarf stars are presented in Figure 1. Spectra of other stars observed can be found in Dupree *et al.* (1979), Hartmann *et al.* (1979), Hartmann, Dupree, and Raymond (1980, 1981) and Dupree and Hartmann (1980). The list of observed stars is presented in Table 1.

Short wavelength emission line fluxes are reported in Table 2, along with exposure times. Wavelengths given in the tables indicate the observed point of peak flux; Harvel, Turnrose, and Bohlin (1979) have found that such exposures typically have offset errors $\sim \pm 4.1$ Å extending throughout the spectrum, as well as random stretching or compressing errors in the dispersion solution $\sim$ 2.2 Å. Thus, line identifications can be difficult, particularly when the solar spectral analogy is not appropriate. We have indicated the most probable identification in Table 2.

Except where noted, all exposures were made with the large aperture, in order to obtain absolute photometry. A least-squares fit has been used to determine the background level, with obvious lines in the spectrum deleted. This procedure is somewhat subjective due to the difficulty of interpreting weak emission at low dispersion as either lines or continuum, or establishing continuum levels in regions with substantial and variable line blanketing. However, some continuum subtraction is necessary, particularly in the earliest spectral types for which continuum and scattered light contributions are important. For stars earlier than $\sim$ G5, the continuum is sufficiently strong that lines longward of 1500 Å are not easily detectable. The continuum corrections are small for types later than K0. The background correction for N V λ1240 is also often significantly uncertain because of the presence of the strong Lyα geocoronal line emission in the large aperture.

With a background fit, it is also possible to integrate the residual flux in a specified wavelength interval in order to obtain an upper limit to a line of interest. Upper limits measured in this way are also listed in Table 2. This procedure is not very precise, but it yields an indication of the meaning of a nondetection. In cases where the residual from the baseline was essentially zero, we have adopted an upper limit based on typical upper limits from other spectra of comparable exposure times. When the flux was negative or the spectrum saturated, no estimate is given.

We have attempted to indicate the repeatability of the spectra in the following manner. Holm's (1979) data suggest that the repeatability of medium to optimally exposed spectra is $\sim 3.2\%$ (1 σ) in 25 Å bins. We have tentatively adopted a minimum error $\sim 6.5\%$ (1 σ) in a 6 Å resolution element and then assumed that the signal-to-noise ratio varies approximately as the square root of the signal strength. Comparisons of this recipe for estimating errors with a few repeated emission line exposures yield reasonable agreement (for fairly well exposed spectra with low background). The quality of the listed fluxes has therefore been denoted by the letters A, B, and C, indicating estimated errors $< 20\%$, $< 40\%$, or $\sim 2\mathbf{x}$, respectively. In some cases uncertainty in the background subtraction or effects of high particle radiation backgrounds have been taken into account in increasing the estimated error. Comparisons of different results indicate that the short wavelength absolute calibration may be accurate to $\sim 10\%$, except at the shortest wavelengths (Bohlin and Snijders 1978; Bohlin and Holm 1980; Bohlin *et al.* 1980).

Long wavelength (LWR) exposures in the high dispersion mode were taken to obtain Mg II (λ2800) fluxes. Correction for the echelle blaze response was made by dividing by the function

$$R = (1 + ax^2)(\sin x/x)^2 ,$$

where $x = \lambda - \lambda_m$, $\lambda_m = K/m$ is the central wavelength of order m, and a and K are suitably chosen constants. We adopted the values $a = 0.10$ and $K = 230{,}975$ for orders 82 and 83, as suggested by Beeckmans and Penston (1979). This choice of constants appears to provide acceptable flattening of the blaze as indicated by tests with flat continuum objects. The results of such reductions are shown in the Mg II spectra presented in Figure 2. Some of the profiles have been commented upon in earlier papers; we defer discussion of profile information to a later paper.

The Mg II spectra were calibrated using the results of Bohlin and Holm (1980) for low dispersion spectra by computing the ratio of high dispersion format sensitivity to that at low dispersion. The continuous spectra of the early-type primaries of HD 153919 (3U 1700–37) and HD 77581 (Vela X-1) were used to calculate this ratio. Although these stars are not strictly constant, their photometric variations at λ2800 Å are expected to be $< 10\%$, based on optical data. Furthermore, the low

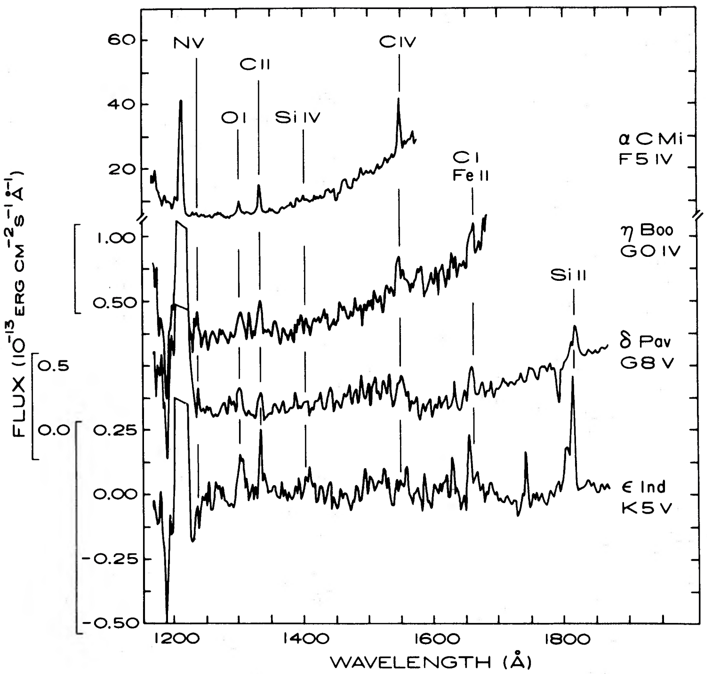

FIG. 1*a*

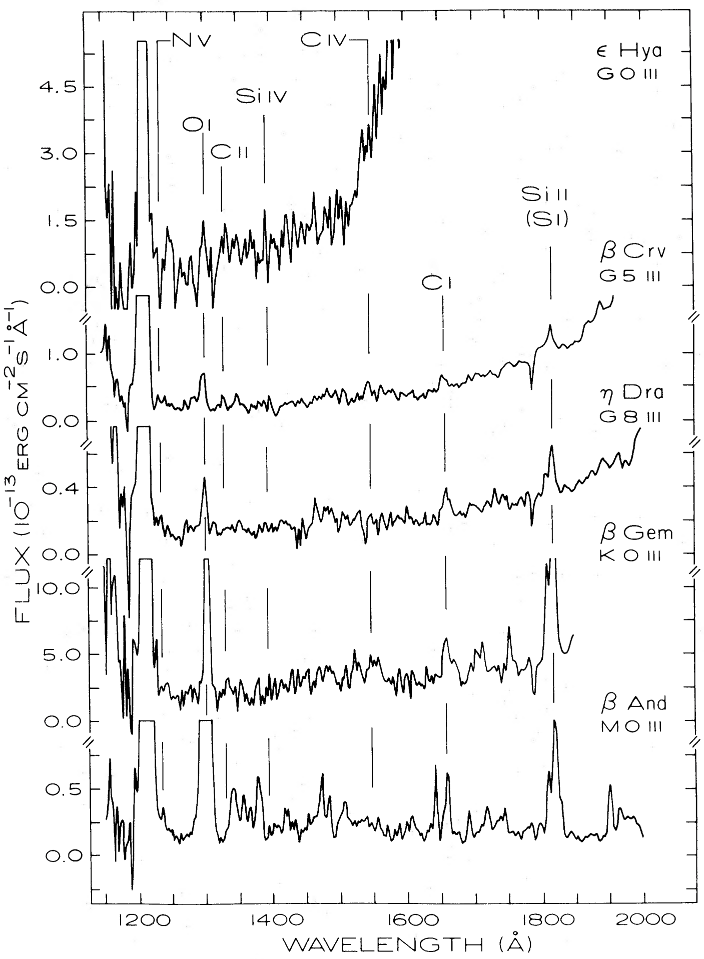

FIG. 1*b*

FIG. 1.—Short wavelength (SWP) spectra of selected stars not presented in previous publications. The spectrum of α CMi has been taken from Brown, Jordan, and Wilson (1979) for comparison.

TABLE 1

STARS IN SURVEY

Name	Sp Type[a,b]	V	$B-V$[a]	$V-R$	T_{eff}	SWP	t (min)	LWR	t (min)	M_v	C IV/solar
					Supergiants						
α UMi[c]	F8 Ib	2.02	0.60	0.49	6150	3636	30	...	...	−4.7	<0.2
δ CMa	F8 Ib	1.84	0.67	0.51	6150	3628	10	...	...	−4.7	<1.1
β Aqr	G0 Ib	2.87	0.84	0.61	5800	3646	60	3207	15	−4.7	1.2
α Aqr	G2 Ib	2.93	0.97	0.66	5500	3587/ 3610	70/ 120	3177	15	−4.7	1.1
ζ Cyg[d]	G8 II	3.20	0.99	0.70	(4960)	3611	120	...	...	−2.1	<0.4
α UMa[e]	K0 III	1.79	1.07	0.81	4720	1564	45	...	...	+0.5	<0.07
β Ara[f]	K3 Ib	2.84	1.46	...	4300	1576	100	1517	90	−4.6	<0.04
α TrA	K4 II	1.91	1.44	...	4100	8570	60	7307	12	−2.2	0.09
λ Vel	K5 Ib	2.21	1.65	1.24	3750	1573	60	3208	20	−4.6	<0.07
					Giants and Subgiants						
ε Hya	G0 III	3.38	0.68	0.60	(5850)	3626	60	3194	30	+1.2	<0.5
β Crv	G5 III	2.64	0.88	0.88	5010	1572/ 3585	90/ 90	1512	10	0.7	0.5
μ Her	G5 IV	3.42	0.75	0.53	(5335)	4715	70	...	...	+3.1	0.8
η Dra	G8 III	2.74	0.91	0.61	4870	1551/ 3597	45/ 160	3209	8	+0.6	<0.14
λ And[g]	G8 III–IV	3.82	1.02	0.78	4870	3613	75	...[i]	5	+3.1	12.6
77 Tau	G8 III	3.83	0.95	0.71	4870	6871	180	5840	20	+0.6	0.9
δ Tau	K0 III	3.76	0.99	0.73	4720	6879	180	5845	20	+0.5	<0.15
HR4665[e]	K0 III	5.40		...	4980	1565	60	3210	30	+0.5	18.0
σ Gem[g]	K1 III	4.17	1.12	0.92	4580	1872/ 6873	70/ 20	5841	6	+0.4:	9.1
β And[h]	M0 III	2.05	1.57	1.24	3660	3647	60	3165	6	−0.4	<0.13
					Dwarfs						
ξ Boo A	G8 V	4.54	0.77	0.63	5440	1558/ 1559	45/ 160	3211	15	+5.5:	10.4
δ Pav	G8 V	3.56	0.76	0.61	5440	3586	120	3160	20	+5.5:	<0.46
ε Ind	K5 V	4.69	1.06	0.88	4400	1577	60	1518	15	+7.3	<0.33
EQ Peg	dM 3.5e– dM 4.5	10.38	1.56	...	...	3612	180	...	...	+11.0:	23.0
VW Cep[g]	dG 2	7.10	0.86	...	...	...[i]	~10	...[i]	~25	5.7	47.0
44 Boo[g]	dG 1	4.80	0.85	...	...	...[i]	~30	...[i]	~15	5.25	120.0

[a] Johnson *et al.* 1966.
[b] Morgan and Keenan 1973.
[c] Variable.
[d] Wilson's K line width gives anomalously low luminosity.
[e] K0 IIIa.
[f] Small aperture.
[g] Close binary.
[h] M0 IIIa.
[i] Several exposures.

dispersion and high dispersion exposures compared were taken a small fraction of the orbital period apart. These comparisons indicate a ratio of low dispersion to high dispersion sensitivity at 2800 Å of $r \approx 95 \pm 5$. A further exploration of this ratio, measuring the Mg II line flux of λ And at low and high dispersion, resulted in $r = 100$. We have therefore adopted $r = 95$ for the fluxes reported here. The recent calibration by Cassatella, Ponz, and Selvelli (1980) suggests $r \sim 100$ for this wavelength region; our fluxes should be multiplied by 1.05 to convert to this scale. The recent results of Basri and Linsky (1979) for Mg II used $r \sim 135$, and so their fluxes must be reduced by this factor in order to put them on the same scale. It appears that the Basri-Linsky calibration may be incorrect due in part to an exposure timing error (Stencel and Ayres 1980).

The Mg II fluxes listed in Table 3 are integrals of the total power between the h_1 and k_1 minimum points. Model calculations by E. Avrett (1980, private communication) indicate that this is the correct measure of chromospheric radiative losses for the stars studied here, rather than the difference from a radiative equilibrium model as suggested by Linsky and Ayres (1978), and is simpler to define; the difference is small in any event.

1982ApJ...252..214H

TABLE 2

FLUXES OBSERVED WITH *IUE*

α UMa SWP 1564 $t = 2700$		α UMi SWP 3636 $t = 1800$		δ CMa SWP 3628 $t = 600$		ε Hya SWP 3626 $t = 3600$	
λ1236–1244	<1.7	λ1305	2.25 C	λ1305	4.2 C	λ1301	3.5 A
1307	9.0 A	1346–1356	1.73 C	1327–1335	<0.7	1334	1.5 B
1336–1346	<0.4	1543–1556	<0.73			1392–1413	<1.5
1388–1407	<1.1						

β Crv SWP 1572 $t = 5400$		β Crv SWP 3585 $t = 5400$		η Dra SWP 1551 $t = 2700$		η Dra SWP 3597 $t = 9600$	
λ1307	3.75 A	λ1304	3.99 A	λ1234–1247	<1.4	λ1235–1246	<0.6
1336	0.53 B	1328–1336	0.33 C	1296	0.71 B	1304	2.58 A
1388–1404	<0.59	1387–1408	<0.26	1307	2.57 A	1331–1344	<0.08
1546	2.02 B	1549	0.88 C	1357	0.71 C	1387–1405	<0.34
1648–1664	1.62 B	1656	0.60 C	1543–1556	<0.7	1544–1561	<0.41
1811b	1.82 B	1816b	2.79 B	1656	0.53 C	1662	1.86? B
				1802	0.24 C	1811	1.2 C
				1814	1.00 C	1819	2.5 C

δ Pav SWP 3586 $t = 7200$		ε Ind SWP 1577 $t = 3600$		μ Her SWP 4715 $t = 4800$		ζ Cyg SWP 3611 $t = 7200$	
λ1300	0.43 B	λ1308	1.03 B	λ1295–1309	<0.08	λ1304	0.97 B
1332	0.75 B	1337	1.31 B	1333	0.5 C	1333	0.33 C
1541–1554	<0.61	1549–1565	<0.45	1540–1556	<0.9	1540–1557	<1.1
1639–1652	<0.1	1661	1.24 B	1655	0.88 B	1658	1.79 A
1657	1.06 B	1809	1.04 B	1805	0.97 B	1688–1706b	1.42 A
1815b	1.0 C	1819	2.31 B	1815	3.62 A	1747?	1.01 A
						1811	0.29 B
						1819	1.00 A

ξ Boo A SWP 1558 $t = 2700S$		ξ Boo A SWP 1559 $t = 9600$		EQ Peg SWP 3612 $t = 10800$	
λ1239	0.97 B	λ1238	0.95 B	λ1239	0.75 B
1307	2.80 A	1304	2.46 A	1305	0.70 B
1338	3.70 A	1333	3.52 A	1335	1.92 A
1397	1.55 B	1391	1.66 A	1393	
1404	0.43 C	1399	1.19 A	+1404	1.04 B
1549	7.0 A	1544	5.20 A	1550	3.68 A
1564	1.30 B	1558	0.65 B		
1640	2.75 A	1637	3.30 A	1642	0.94 B
1656	1.58 B	1655	2.57 A	1660	0.99 B
1805	3.24 A	1804	2.98 A	1812	0.49 B
1814	6.18 A	1811 OE		1820	0.69 B

σ Gem SWP 6872 $t = 4200$		σ Gem SWP 6873 $t = 1200$	
λ1175	15.2 C	λ1237	12.3 A
1237	11.4 A	1287–1298b	5.1 C
1304 OE		1304	34.3 A
1336	17.6 A	1336	15.8 A
1357	3.57 A	1357	2.89 B
1394	7.73 A	1394	10.2 A
1402	6.39 A	1404	8.89 A
1551	31 A	1548	23.6 A
1641	11.8 A	1641	11.8 A
1660	9.67 A	1660	11.4 A
1668	3.45 A	1670	6.34 B
1751	2.07 A	1752	3.31 B
1808	7.38 A	1808	5.53 B
1819	16.3 A	1819	16.2 A
1851–1867b	1.80 A	1851–1867b	14.24 B
1892	10.8 A	1892	9.86 A
1909b?	4.21 A	1909	3.47 B

TABLE 2—*Continued*

β And SWP 3647 $t = 3600$			
λ1296	7.76 B	λ1653	1.06 B
1304 OE		1661	1.68 B
1343b	2.06 B	1693	0.58 B
1349–1371b	2.28 B	1717b	1.73 B
1378b	2.12 B	1730–1741b	0.90 B
1421b	1.16 B	1746	1.12 B
1427–1437b	0.85 B	1811b	2.09 B
1474	2.55 A	1818b	4.28 A
1485	1.33 B	1829b	0.84 B
1506b	2.54 B	1901	1.88 A
1511–1543b	3.04 B	1909–1925b	2.18 B
1543–1557	0.87 B	1925–1933b	1.50 B
1642	1.57 B	1933–1949b	1.79 B

NOTE.—Fluxes in units of 10^{-13} ergs cm^{-2} s^{-1}. b = blend. OE = overexposed. A = estimated error < 20%; B = error < 40%; C = error ~ 2x.

III. ANALYSIS OF SOLAR TYPE LINES

In Table 3 we present emission-line surface fluxes averaged over the stellar disk, F_*, for solar type lines. We use units of the quiet Sun surface fluxes (G. Rottman, as quoted in Linsky *et al.* 1978) in order to facilitate comparison. The conversion factors from flux observed at the Earth to surface fluxes have been derived using the $V-R$ colors and the Barnes-Evans (1976) relation for the W UMa stars, where parallaxes and known stellar radii from eclipse data have been used, and for β Ara and α TrA, for which we used the Barnes-Evans relation for $B-V$. Fluxes at the Earth $f_\oplus$ for objects not in Table 1 can be calculated using the given angular diameter factor α from the formula $f_\oplus = \alpha(F_*/F_\odot) \times F_\odot$. No corrections have been applied for interstellar extinction; such corrections might be important for supergiants but are uncertain.

For convenience, the fluxes from α Aqr, β Aqr, α TrA, and λ Vel, which have already been reported (Hartmann, Dupree, and Raymond 1980, 1981) are included. The fluxes for ξ Boo and EQ Peg, having been corrected for the ITF error, supersede previously reported fluxes (Hartmann *et al.* 1979); the changes are not large enough to affect the conclusions of that paper.

a) *Temperature Structure of Outer Atmospheres*

The general results of our survey can be seen at a glance from Figure 3, where the line fluxes for various stars are plotted in a sequence of increasing line excitation, with (approximate) temperatures of formation. The fluxes have been normalized in units of solar surface fluxes in the various lines. Downward pointing arrows indicate upper limits.

We draw the following conclusions from the entire data set in Tables 2 and 3, as highlighted by Figure 3.

1. High temperature species (characteristic of solar TR lines) vary more widely than the chromospheric losses (represented by Mg II *h* and *k*). In active stars, the enhancement of surface flux (averaged over the entire stellar surface) increases with increasing temperature of line formation, in a manner typical of solar active regions. This conclusion was suggested previously (Hartmann *et al.* 1979). He II λ1640 is enhanced over the general temperature progression; this may be the effect of coronal photoionization (Hartmann *et al.* 1979; see below). These patterns suggest that active stellar behavior is different from solar activity only in degree and not in kind.

2. Mg II emission is well correlated with high temperature ion line fluxes. This can break down in close detail (e.g., HR 4665 vs. ξ Boo), but the overall trend is apparent. Similar results have been obtained independently by Ayres, Marstad, and Linsky (1981). Standard theory suggests that different mechanisms are required to heat chromospheric and coronal regions (e.g., Stein and Leibacher 1980), but Figure 3 clearly indicates that these mechanisms are related.

3. Upper limits to high temperature (C IV) emission from *IUE* observations are usually surface fluxes ~ 10^{-1} to 10^{-2} of solar values. However, if one compares the relative amounts of low and high temperature emission, the difference is less dramatic. For example, in β And (Fig. 3), the upper limit to C IV emission is only a factor of 3 to 10 below the Mg II flux, relative to the dsitribution of emission in the quiet Sun. Thus the *IUE* limits are not terribly stringent on the *shape* of the emission measure curve, because the stars with low limits on hot emitting gas also tend to have weak chromospheric emission. We also note that the G8 III star η Dra, for which we have an upper limit of ~ 10^{-1} of the quiet Sun surface flux in TR lines, has apparently been detected in X-rays using the *Einstein* satellite at a level ~ 10^{-1} of quiet Sun X-ray flux (Vaiana *et al.* 1981).

b) *Line Ratios and Physical Conditions*

The solar transition region can be described in a plane parallel geometry at approximately constant pressure. While there is no *a priori* assurance that constant pressure transition regions exist on other stars, particularly on low gravity objects, the similarity of surface fluxes to solar values makes this assumption plausible for most stars.

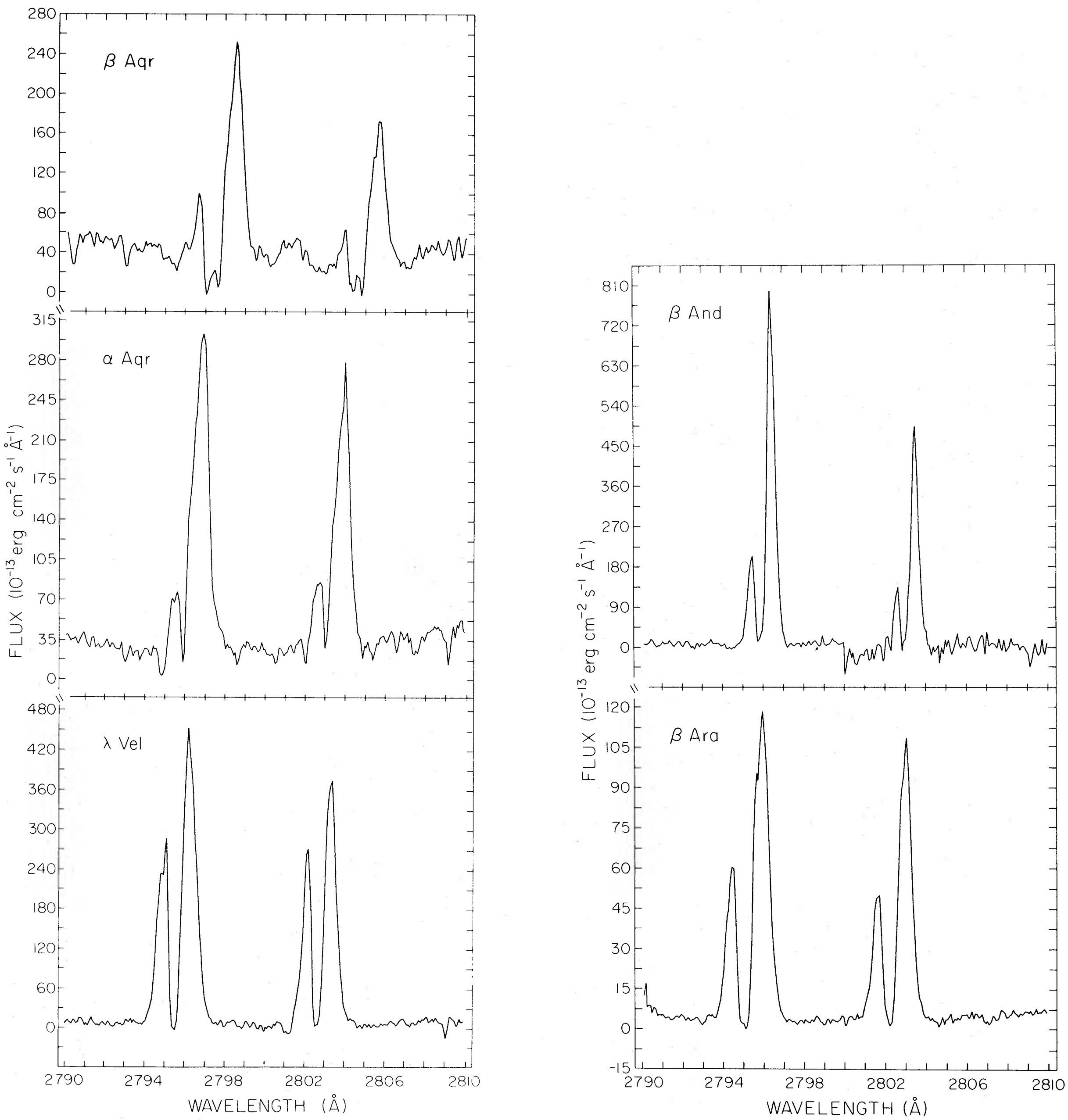

FIG. 2a

FIG. 2b

FIG. 2.—High dispersion, long wavelength (LWR) spectra of the Mg II emission lines of most of the program stars

Theories of conductively dominated transition regions in plane parallel, constant pressure environments generally result in emission measures which scale linearly with the pressure (Haisch and Linsky 1976; Rosner, Tucker, and Vaiana 1978). These models agree reasonably well with empirical determinations of the differential emission measure as a function of temperature for $T > 1 \times 10^5$ K (Withbroe and Gurman 1973), but do not match well below this temperature (cf. Vaiana and Rosner 1978) where the great majority of ions observable with *IUE* are concentrated. Thus we have no established theory to test for most lines, and are generally restricted to solar analogies.

The line fluxes of solar active regions (Dupree *et al.* 1973) and active dwarf stars (Hartmann *et al.* 1979) show that the emission measure profile is enhanced at high temperatures relative to the quiet Sun. A plausible upper limit to the enhancement of high temperature material

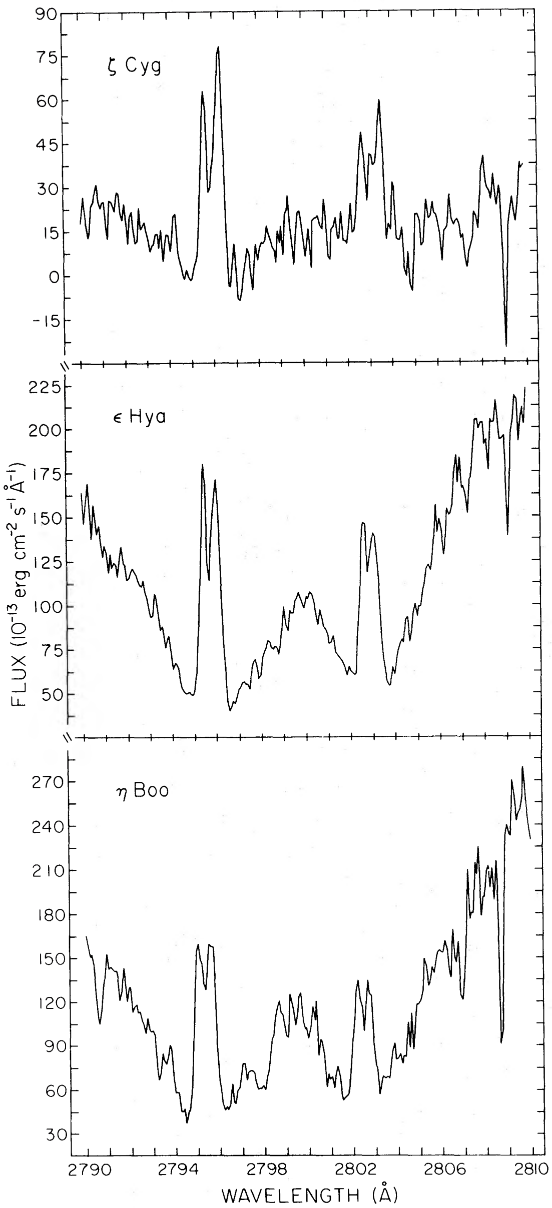

FIG. 2c

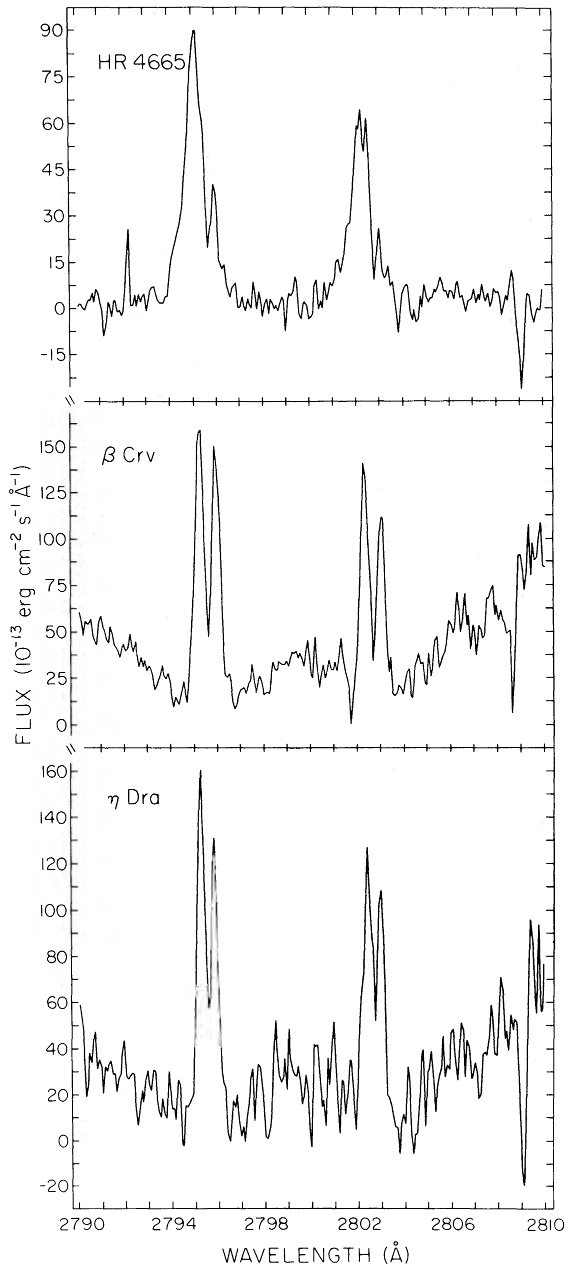

FIG. 2d

can be derived by assuming that conduction from the corona is so strong that the conductive flux is essentially constant (cf. early solar modeling by Athay 1966 and Dupree 1972). This results in a differential emission measure $Q = N_e^2(dT/dh)^{-1} \propto T^{1/2}$. We have integrated the N V and C IV fluxes in a model transition region with $Q \propto T^{1/2}$, using the ionization equilibrium of Vernazza and Raymond (1979). The result indicates that such a region would produce an enhancement in the *ratio* of N V/C IV by a factor of 4 over the average solar ratio, or a net N V/C IV flux ratio ~ 0.6.

Inspection of Table 2 indicates that the only stars approaching such a ratio are the hybrid stars α Aqr and β Aqr, which have N V/C IV ratios of 0.66 and 0.54, respectively. (Line identification at low dispersion is difficult, but the fact that other luminous stars like λ Vel and β And exhibit no λ1240 flux at a comparable order of magnitude strongly indicates that λ1240 is indeed N V, especially when C IV and Si IV are also present.) The flux ratios for these stars appear to be accurate; two exposures of α Aqr agree to the 10% level in N V, C IV, and Si IV (Hartmann, Dupree, and Raymond 1980). The hybrid star α TrA has a

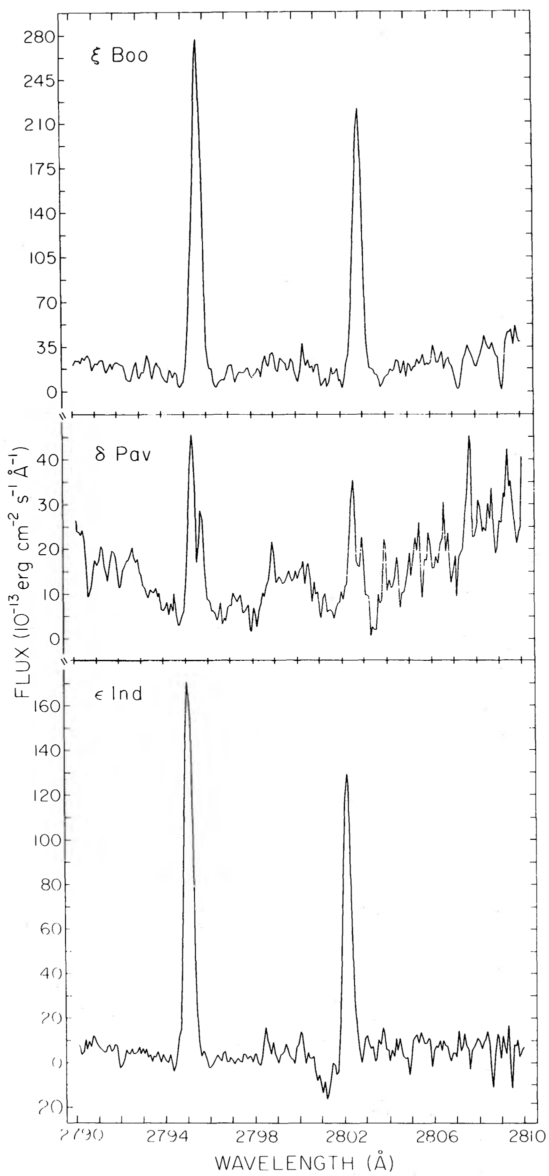

FIG. 2e

similarly enhanced ratio of N v/C IV relative to the Sun, although the averaged surface fluxes are much lower than solar. In the case of α TrA, however, high dispersion exposures have shown that the lines of solar transition region ions like C IV, C III, and Si III are much wider in the Sun; this has been interpreted to mean that these lines reflect wind expansion (Hartmann *et al.* 1981). The enhancement of N v may be due to the peaking of coronal emission measures at $\sim$ few $\times 10^5$ K. We note that while the N v surface fluxes in α Aqr and β Aqr are $\sim 4 \times$ solar, Ayres *et al.* (1981) have found upper limits to the X-ray fluxes roughly a factor of 2 below the average quiet Sun. In any event, the physical conditions in the hybrid stars appear far from the constant pressure, hydrostatic case assumed above. The other active stars have N v/C IV ratios $\lesssim 0.44$, and C IV enhancements $\gtrsim$ Si IV, and so are consistent with the notion of conductively dominated transition regions.

c) *Ratios of X-ray to UV emission*

Walter *et al.* (1980) have applied the loop models of Rosner, Tucker, and Vaiana (1978) to X-ray emission from RS CVn variables. Although Walter *et al.* (1980) modeled the X-ray emission with a single temperature, the loop models predict a well defined distribution of emission measure Q as a function of T. We may make a crude estimate of the form of the differential emission measure $Q(T)$ by looking at the ratio of emission measures required to produce the X-ray and N v emission. For simplicity, we assume that N v is formed at $T = 2 \times 10^5$ K and the X-rays come from a single temperature of 1×10^7 K (Walter *et al.* (1980). Then we may examine the ratio $\log y = \log [TQ(X)/TQ(\mathrm{N\ v})]$. Since the loop models predict $TQ(T) \propto T$, we expect $\log y \sim 1.7$.

In Figure 4 and in Table 4 we exhibit the N v and X-ray emission measures for six stars. Generally speaking, this crude estimate indicates adequate agreement ($\sim$ factor of 2) with the loop model, except for the long period RS CVn star σ Gem, which has substantially enhanced emission measures at low temperatures. Further tests should be made, especially by seeing if $TQ(T) \propto T$ can fit the X-ray data as well as single-temperature fits.

d) He II *Fluxes and Coronal X-ray Emission*

Hartmann *et al.* (1979), following the solar work of Raymond, Noyes, and Stopa (1979), showed that enhancements of He II λ1640 in the active dwarfs ξ Boo A and EQ Peg could be interpreted as the result of excess recombination following photoionization by coronal X-ray radiation. This inference was consistent with the X-ray fluxes for ξ Boo reported by Walter, Charles, and Bowyer (1978). Here we test the hypothesis further for several other stars.

As described by Hartmann *et al.* (1979), the He II λ1640 line may be partially formed by recombination following photoionization by coronal EUV radiation. Though the uncertainties are fairly large, the λ1640 flux gives at least a crude method for comparing X-ray and UV observations. On the basis of the ratios of the surface flux of C IV λ1550 to the quiet Sun, we divide the stars into "quiet," "active," and "superactive." This is necessary because collisional excitation cannot be neglected in computing the total He II flux, and because coronal temperatures vary. Following the studies of Raymond, Noyes, and Stopa (1979) in assessing the formation of He II emission in solar regions of differing activity, we assume that the fractions of λ1640 emission due to recombination are 0.3, 0.6, and 0.8, for quiet, active, and superactive stars, respectively. We then use the calculations described by Raymond, Noyes, and Stopa (1979) and the X-ray emission code of Raymond and Smith (1977; modified to correct dielectronic recombination rates for autionization to excited levels) with solar abundances (Withbroe

TABLE 3

SURFACE FLUX RATIOS $F_*/F_\odot$ (SOLAR TYPE LINES)

Star, Sp Type	N V	C IV	Si IV	He II	C II	O I	C I	Si II	Mg II
δ CMa, F8 Ib (7.59-17)	...	...	...	...	<0.2	<1.4	...	...	...
α UMi, F8 Ib (5.94-17)	...	<0.2	...	...	<0.2	<0.8	...	...	...
β Aqr, G0 Ib (4.36-17)	4.4	1.2	2.3	<1.9[a]	0.7	8.5	0.8	1.1	0.55
α Aqr, G2 Ib (5.03-17)	4.9	1.1	2.2	<3.1[a]	0.8	15	1.0	1.1	0.66
ζ Cyg, G8 II (4.60-17)	...	<0.4	...	...	≲0.15	0.53	0.73	0.18	...
α UMa, K0 II (2.60-16)	...	...	...	...	<0.03	0.87	...	...	...
β Ara[b], K3 Ib (4.01-16)	...	...	...	...	(0.01)	(0.5)	(0.01)	(0.02)	(0.043)
α TrA, K4 II (8.97-16)	0.4	0.09	0.16	<0.16[a]	0.06	>1.9	0.09	0.10	...
λ Vel, K5 Ib (9.66-16)	...	<0.07	<0.27	0.27[a]	<0.15	1.3	0.02	0.07	≲0.046
ε Hya, G0 III (2.67-17)	...	...	<2.2	...	1.2	3.3	...	...	0.64
μ Her, G5 IV (1.92-17)	...	<0.8	...	...	~0.5	<0.1	0.9	1.5	...
β Crv, G5 III (5.39-17)	...	~0.5	<0.3	...	~0.17	1.8	~0.4	0.27	0.32
η Dra, G8 III (4.92-17)[c]	...	<0.14	<0.27	...	<0.04	1.5	~0.5	0.5	0.33
77 Tau, G8 III (3.08-17)	2.8	0.9	2.0	2.2	0.9	2.7	0.9	0.74	0.50
δ Tau, K0 III (3.21-17)	...	...	<0.35	...	0.2	1.6	0.5	0.44	0.28
λ And, G8 III–IV (3.59-17)	12.4	12.6	8.0	32	7.0	26	6.0	4.3	3.2
HR 4665, K0 III[d] (5.03-18)	40	18	20	32	13.4	22	5.8	4.4	1.6
σ Gem, K1 III (4.49-17)	30	9.1	12.2	28	8.5	19	4.1	3.3	...
β And, M0 III (1.12-15)	...	<0.013	...	0.11	<0.027	OE	0.028	0.038	0.030
44 Boo G1 V (2.92-18)	200	120	83	240	54	38	...	...	...
VW Cep, G5 V+K1 (1.44-18)	110	47	28	65	26	16.0	14.4	14.1	...
ξ Boo A, G8 V (1.01-17)	11.2	10.4	9.4	23	7.8	6.5	3.9	5.8	2.2
δ Pav, G8 V (2.31-17)	...	<0.46	...	<0.33	0.71	0.47	0.87	~0.27	0.20

TABLE 3—*Continued*

Sp Type	N v	C iv		He ii	C ii	O i	C i	Si ii	Mg ii
ϵ Ind, K5 V (2.37-17)..........	...	$\lesssim$0.33	...	...	1.2	1.1	1.0	0.9	0.47
EQ Peg[d], dM3.5e + dM4.5 (2.92-18)..........	30	23	14	25	14	6.0	6.4	2.5	...
$F_{\odot}$[e]...............	8.5 + 2	5.8 + 3	2.58 + 3	1.3 + 3	4.6 + 3	4.0 + 3	5.3 + 3	1.6 + 4	1.25 + 6

[a] Most of this flux is probably not He ii, as determined from high-dispersion studies (Brown and Jordan 1980; Hartmann, Dupree, and Raymond 1981).
[b] Small aperture.
[c] Flux ratio factor α (see text).
[d] Surface fluxes assume only contribution from primary.
[e] In ergs cm^{-2} s^{-1}; the notation 8.5 + 2 implies $8.5 \times 10^{+2}$.

1976) to predict X-ray fluxes. We use the effective area curve of Giacconi *et al.* (1979) to predict counts per second for the *HEAO 2* (*Einstein*) IPC, and we predict the flux at the Earth in the 0.12–2.7 keV bandpass for comparison with *HEAO 1* LED observation. Predictions are made for three models: a single temperature (2×10^6 K, 3×10^6 K, and 10^7 K) for quiet, active, and superactive stars respectively; and logarithmic emission measures $TQ(T) \propto T$ and T^2 up to temperatures $T_{max} = 2.5 \times 10^6$ K, 4×10^6 K and 5×10^7 K for quiet, active, and superactive stars respectively. If thermal conduction balances radiative emission, as in loop models (e.g., Rosner, Tucker, and Vaiana 1978), $TQ \propto T^1$. Constant conductive flux results in $TQ \propto T^{1.5}$, and this is typical of the quiet Sun (e.g., Athay 1966). A steeper gradient, $TQ \propto T^3$, is seen in solar active regions (Doyle and Raymond 1981).

The effects of these assumptions are shown in Table 5. As can be seen from Table 6, the observed fluxes are within a factor of 2 or 3 of predictions and generally underestimate the flux. Besides uncertainties in the theory and the λ1640 fluxes, the comparison is hindered by the lack of simultaneous measurements and the fact that some assumed spectral shape (in this case a 10^7 K bremsstrahlung spectrum) was used to derive X-ray flux from count rate for the *HEAO 1* measurements. In view of these problems, preliminary agreement of a factor of 2 to 3 may be considered reasonable, pending more detailed

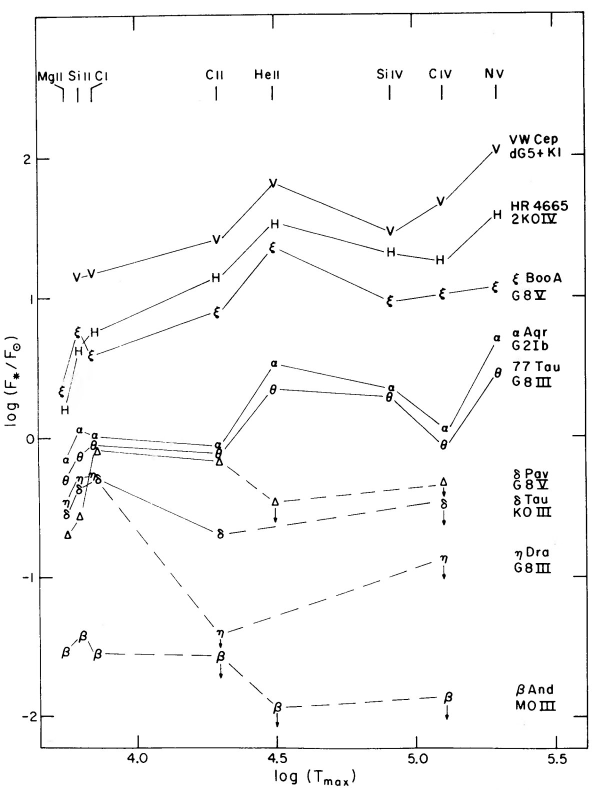

FIG. 3.—Emission line surface fluxes for several representative stars. The lines are arranged with a rough indication of their expected temperature of formation assuming collisional ionization and excitation. The surface fluxes are normalized in units of the average Sun surface fluxes, as described in the text. Arrows indicate upper limits.

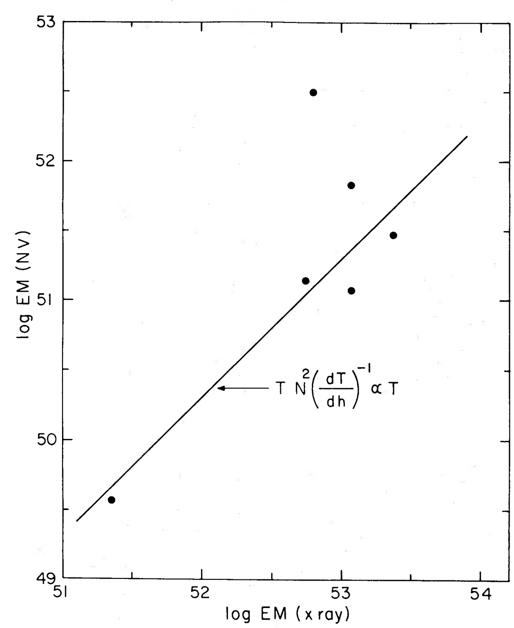

FIG. 4.—Plot of emission measures determined from the N v λ1240 emission ($T \sim 2 \times 10^5$ K) vs. high-temperature ($T \sim 10^7$ K) emission measures derived from X-ray fluxes. The straight line indicates the relationship predicted by standard TR-coronal models (see text).

TABLE 4

CORONAL AND TR EMISSION MEASURE RATIOS

Star	L_x (ergs cm^{-2} s^{-1})	d(pc)	$EM(X)$(cm^{-3})	$f_{\mathrm{N\,V}}$ (ergs cm^{-2} s^{-1})	$EM_{\mathrm{N\,V}}$ (cm^{-5})	log Y[a]
α Aur	4×10^{30}	14	1.2×10^{53}	...	6.8 + 51[b]	1.25
σ Gem	2.1×10^{30}	59	6.3×10^{52}	1.14–12	3.2 + 52	0.30
HR 4665	8×10^{30}	47	2.4×10^{53}	1.7 –13	3.0 + 51	1.90
λ And	1.9×10^{30}	24	5.7×10^{52}	1.24–12	1.4 + 51	1.61
σ CrB	4×10^{30}	21	1.2×10^{53}	3.5 –13	1.2 + 51	1.99
ξ Boo A	7.7×10^{28}	6.9	2.3×10^{51}	0.96–13	3.6 + 49	1.80

[a] $Y = EM(X)/EM(\mathrm{N\,V})$; for $TQ \sim T$, log $Y \sim \log(10^7/2 \times 10^5) = 1.7$.
[b] Effective emission measure taken from Haisch and Linsky 1976.

studies. However, a few stars are clearly discrepant. The X-ray fluxes for δ Pav are much higher than predicted and may indicate a higher value of $T_{\max}$. The predicted X-ray fluxes for σ Gem and α Aur are too high. This result may indicate the presence of intermediate temperature ($T \sim 5 \times 10^5$ K) gas in these systems which can efficiently photoionize He I but will not affect the observed X-ray fluxes. The upper limits for α Aqr and β Aqr are well above the X-ray upper limits (Ayres *et al.* 1981); however, most of the λ1640 flux observed at low dispersion probably comes from lines other than He II (Brown and Jordan 1980; Hartmann, Dupree, and Raymond 1981).

e) *Transition Region Pressures*

Pressures in the transition region and (by extension) at the base of the corona are important quantities in physical modeling. The best method for getting pressures is of course to use a density diagnostic. Unfortunately, the C III/Si III ratio technique suggested by Doschek *et al.* (1978) suffers from the neglect of charge exchange processes in the Si II/Si III ionization balance (Baliunas and Butler 1980) and the low line intensities, leading to substantially greater uncertainty in the line fluxes.

The C III λ1176/λ1909 ratio is a better density diagnostic, although it is somewhat temperature-sensitive (Nussbaumer and Schild 1979) and subject to nonequilibrium conditions (Raymond and Dupree 1978). Unfortunately, the sensitivity of *IUE* at λ1176 is so low that we have only one star in our sample for which a reasonable estimate of the λ1176 flux can be made, and that is σ Gem.

TABLE 5

PREDICTED RATIO OF X-RAY FLUX TO THE He II λ1640 FLUX[a]

ASSUMED TYPE[b]	EMISSION MEASURE DISTRIBUTION		
	$1T$	T^1	T^2
Q	0.156	0.127	0.141
A	0.486	0.156	0.211
S	0.275	0.185	0.146

[a] In units of IPC counts s^{-1} per 10^{-13} ergs cm^{-2} s^{-1} of He II flux observed at Earth.
[b] Q = quiet, A = active, S = superactive; see text.

The line ratio indicates a pressure of $\sim 10^{-1}$ dyne, that is, close to the average Sun P_{TR}, assuming temperatures $\sim 5 \times 10^4$ K and using the results of Nussbaumer and Schild (1979).

Since models of constant pressure, conductively dominated transition regions have emission measures that scale linearly with the pressure (Haisch and Linsky 1976; Rosner, Tucker, and Vaiana 1978), it suggests that lower limits to P_{TR} may be estimated from the surface fluxes listed in Table 2 (although the loop models do not explain the X-ray to N V emission measure ratio for σ Gem as described above). However, application of this principle results in a pressure for σ Gem that is $\sim 10 \times$ solar values, strongly discrepant with the C III density diagnostic. Either standard TR models are not applicable or inhomogeneities in the transition region account for this discrepancy.

IV. CHROMOSPHERIC AND CORONAL ACTIVITY IN THE H-R DIAGRAM

a) *Dependence of Fluxes on Stellar Parameters*

In Figure 5 we present the Mg II surface fluxes of the program stars plotted as a function of effective temperature. Surface fluxes are found to decay with decreasing effective temperature in a fashion consistent with the observations of Basri and Linsky (1979); the dashed line is the mean trend of their data (for the *k* line alone). It is also apparent that a wide range of chromospheric activity is present at a given position in the H-R diagram, as indicated by Ca II observations (cf. Wilson 1966). This is inconsistent with theories of acoustic energy generation (cf. de Loore 1970; Renzini *et al.* 1977), as remarked by other investigators (Basri and Linsky 1979). The strong chromospheric and transition region emission from the M dwarf system EQ Peg AB is also inconsistent with present acoustic theories (cf. Hartmann *et al.* 1979).

Table 2 lists the fluxes of lines in the short-wavelength region of the spectrum. The ratio of total line losses between λ1220 and λ1950 to Mg II radiative losses is also plotted in Figure 3. Because of saturation and interstellar absorption effects, no attempt has been made to include Lyα fluxes. The O I fluxes have also been deleted from the short wavelength total, because in the most luminous stars they really represent Lyβ losses through resonance fluorescence.

TABLE 6

He II λ1640 AND X-RAY FLUXES

STAR	ASSUMED TYPE	PREDICTED IPC[a] 1T	T^1	T^2	OBS. IPC[a]	PREDICTED LED[b] 1T	T^1	T^2	OBS. LED[b]
λ Vel	Q	≤0.05	≤0.05	≤0.06	...	≤0.05	≤0.13	≤0.18	...
β And	Q	≤0.06	≤0.06	≤0.07	...	≤0.06	≤0.16	≤0.21	...
δ Pav	Q	≤0.003	≤0.004	≤0.004	0.018[c]	≤0.003	≤0.010	≤0.013	...
α Aqr	A	≤0.06	≤0.17	≤0.25	<0.01[d]	≤0.13	≤0.28	≤0.50	...
β Aqr	A	≤0.03	≤0.09	≤0.14	<0.01[d]	≤0.07	≤0.16	≤0.28	...
ε Eri	A	3.2	0.9	1.4	0.76[c]	0.69	1.6	2.8	...
77 Tau	A	0.26	0.06	0.11	...	0.06	0.11	0.22	...
ξ Boo	S	0.99	0.99	1.7	...	1.8	1.6	3.0	4.2[e]
λ And	S	4.3	4.3	7.5	...	7.8	7.1	13.0	2.8[f]
HR 4665	S	0.68	0.68	1.2	...	1.2	1.1	2.1	3.4[f]
σ Gem	S	5.2	5.2	8.8	...	9.8	8.7	16.0	5.2[f]
44 Boo	S	2.9	2.9	5.1	1.5[g]	5.3	4.9	8.9	...
VW Cep	S	0.39	0.39	0.67	0.5[g]	0.70	0.65	1.2	...
EQ Peg	S	3.1	3.1	5.3	...	5.6	5.2	9.3	...
α Aur	S	26.0	26.0	44.0	2.3[c]	46.0	43.0	77.0	18[f]
HR 1099[d]	S	5.3	5.3	9.1	...	8.7	7.6	14.0	10[f]
UX Ari[d]	S	2.6	2.6	4.4	...	4.6	4.3	7.7	...

[a] Units: counts s^{-1}.
[b] Units: 10^{-11} ergs cm^{-2} s^{-1}.
[c] Vaiana *et al.* 1981.
[d] Ayres *et al.* 1981.
[e] Walter, Charles, and Bowyer 1978.
[f] Walter *et al.* 1980.
[g] Dupree and Cruddace 1981.

From Figure 3 it is apparent that the short wavelength fluxes generally follow the Mg II fluxes in their decrease with decreasing effective temperature. It is remarkable that while λ Vel and β And have completely different line spectra from hotter stars like α Aqr, ξ Boo, etc., the ratio of radiative losses remains the same at an order of magnitude level. Apart from the possible variation of hydrogen radiative losses, the decrease of Mg II fluxes may be representative of a real change in mechanical energy fluxes in these stars.

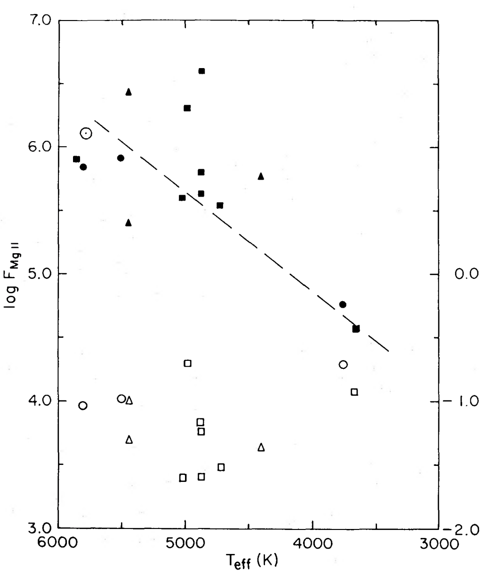

FIG. 5.—Mg II fluxes and their ratio to short wavelength (1215 < λ < 1950) emission line power, as described in the text. *Solid symbols:* Mg II surface fluxes in units of ergs cm^{-2} s^{-1} (left hand scale); *open symbols:* ratio of short wavelength emission fluxes to Mg II fluxes (right hand scale); *circles:* supergiants; *squares:* giants; *triangles;* dwarfs.

The W UMa and RS CVn systems in Table 2 exhibit the highest flux levels. This suggests that rapid rotation, which is tidally enforced for these systems, is the dominant parameter in setting the level of mechanical energy generation (Dupree *et al.* 1979), a suggestion which is consistent with earlier inferences regarding the level of Ca II emission (Kraft 1967; Skumanich 1972; Bopp and Espenak 1977).

We also note that it is difficult to say much about the presence of transition region lines on the earliest-type stars in our sample, because the problem of contrast with the photospheric continuum is so acute.

b) *Existence of Hot Gas in Outer Atmospheres*

We are now able to interpret the presence or absence of C IV emission as detected with *IUE* in terms of the H-R diagram shown in Figure 6. The upper limits are generally ~ 10^{-1} to 10^{-2} of solar surface fluxes; in terms of the general run of emission with temperature, they represent decreases of factors of 3 to 10 below the chromospheric (Mg II) losses.

Among the normal field stars, the presence of C IV in β Crv but not in η Dra suggests a "division" between G8 III and G5 III, while the original Linsky-Haisch dividing line was between G8 III and K0 III. These data suggest that *there is some finite spread in the* H-R *diagram wherein*

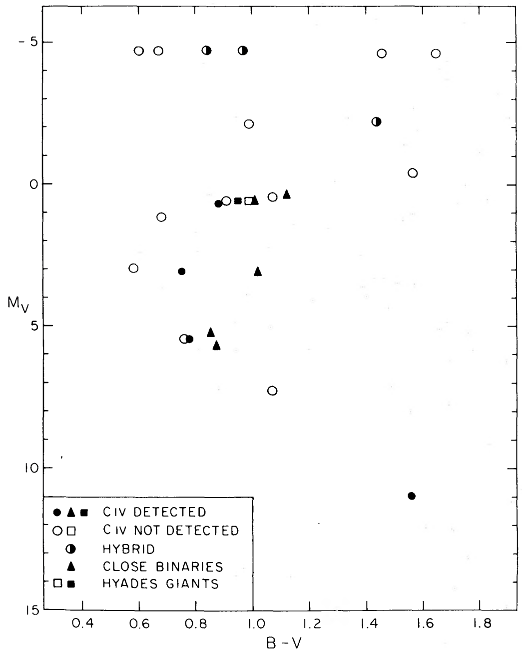

FIG. 6.—H-R diagram indicating detection or absence of C IV emission in the stars studied in this program. Observational selection effects are important in the detection of C IV, as discussed in the text.

strong C IV *emission may or may not be present*, especially since the inclusion of the Hyades giants and the RS CVn systems moves the dividing line to later types in the H-R diagram. The absolute level of mechanical energy deposition affects the existence of transition region lines, in that the more active a star is, the more likely it is to have C IV and N V emission (cf. Fig. 4). Thus the intermingling of "solar" and "nonsolar" chromospheric types appears to be in part a function of stellar parameters other than L and $T_{\rm eff}$, such as rotation.

The β Crv and η Dra results show that a change of a factor of 2 to 3 in surface flux can make the difference between a detection of C IV and an upper limit. The difficulty of measuring a C IV flux can be seen from Figure 1. The reality of the C IV feature in β Crv is decided primarily on the basis of seeing a similar feature in multiple exposures (Table 1). Note that Table 1 may indicate some variability in β Crv, which will also affect detection limits.

We note that Hartmann *et al.* (1979) pointed out that C IV and N V are more enhanced in active dwarf stars than lower excitation lines. Apart from O I, which is probably affected by Lyβ fluoresecence in luminous stars, we see this is generally true of other stars as well, particularly for the W UMa and RS CVn systems. Thus an *IUE* observation is doubly senstivie to high temperature ions in active stars, for reasons of both high average flux, and relative enhancement of high T lines.

The importance of considering sensitivity limits is emphasized by the behavior of the two Hyades giants shown in Table 2 and discussed by Baliunas, Hartmann, and Dupree (1980). 77 Tau has a detectable C IV flux (in a three hour exposure), while δ Tau does not. However, both have been detected in X-rays by Stern *et al.* (1980), and so both presumably have coronae. The X-ray flux from δ Tau is an order of magnitude below that of 77 Tau; the C IV upper limit in Table 2 is clearly compatible with this result. (We cannot completely rule out the possibility of superactive dwarf companions to the giants.)

We also note that our spectra of at least two dwarfs show no clear evidence for C IV emission, even though it seems very likely that they possess hot, solar like outer atmospheres.

In summary, we suggest that it is difficult to determine the *absence* of TR emission at levels much below 10^{-1} × solar. Furthermore, emission at a given spectral type varies widely in strength. The combination of these two effects makes it impossible to define a "sharp" division in the H-R diagram between stars with and without C IV emission.

c) *Overview of Activity in the H-R Diagram*

We have presented a survey of ultraviolet emission line fluxes from late-type stars in which we have made an attempt to quantify the accuracy of the data and identify some observational selection effects that must be recognized before the data can be interpreted properly. The general behavior of solar type activity in the H-R diagram, drawing also on other results, may be summarized as follows.

i) *Chromospheric Activity*

The limits of chromospheric activity are ill-determined. Stars earlier than ~ G0 have such strong photospheric emission at short wavelengths that chromospheric and transition region emission is difficult or impossible to detect. X-ray data (Vaiana *et al.* 1981) now suggest that the canonical "onset of chromosphers" near F5 estimated from optical Ca II observations is primarily a selection effect due to small photospheric contrast. Most chromospheric lines are formed at temperatures ~ 6000–7000 K. This range approaches the radiative equilibrium boundary temperatures for spectral types earlier than about F0. Thus, the "chromospheric" behavior of early F and late A stars might be qualitatively different from that of the Sun without implying changes in the mechanical energy deposition rate.

Our measurements of Mg II surface fluxes generally agree with other investigations (Figure 2; Basri and Linsky 1979; Stencel *et al.* 1980) on two points; the surface fluxes fall with decreasing effective temperature, and there is little segregation by gravity in the G stars. However, we note that all the samples of stars are strongly biased towards the low gravity, luminous stars at the lowest effective temperatures. M dwarfs are extremely underrepresented in general, and not at all in our sample. There appears to be some question as to whether the chromospheric falloff of emission in late spectral types is a function of gravity, at least in part. If chromospheric fluxes are strongly tied to rotation, as is true on the main sequence (Skumanich 1972) and for late subgiants (Hall

1976), then one might expect the largest stars, having the slowest rotation, to have systematically weaker chromospheric activity. Efforts to sample M dwarfs should be pursued in order to resolve this question.

ii) Transition Region and Coronal Activity

We find a close correlation between TR emission and chromospheric activity, with a wide range of emission at a given point in the H-R diagram. The general patterns of emission measure as a function of temperature in high gravity stars have analogous behavior to solar features. A rough comparison of the relative emission measures at 10^7 K and 2×10^5 K is in agreement with simple loop models.

Linsky and Haisch (1979) suggested that transition regions and coronae disappeared suddenly as a function of position in the H-R diagram for luminous late-type stars. We have shown that this cannot be demonstrated clearly primarily because of selection effects due to the limited instrumental sensitivity. In other work we have shown that "hybrid" stars exist, which combine both cold winds and hot (2×10^5 K) gas (Hartmann, Dupree, and Raymond 1980). Thus the *qualitative* nature of the "sharp" division between stellar outer atmospheres suggested by Linsky and Haisch is not correct. Hartmann, Dupree, and Raymond (1981) have presented evidence for wind expansion in the TR line profiles of the hybrid star α TrA and suggest that the maximum coronal temperatures in this object are $< 10^6$ K.

Hartmann and MacGregor (1980) suggested that high temperature coronae disappear in low gravity stars not because of the cessation of heating, but because of enhanced radiative cooling in more massive winds. This suggests that the total radiative losses of stars of different gravity and different mass loss (per unit surface area) may not vary as much as the temperature of the gas. In this regard, the result of Figure 5 is worthy of note. It suggests that radiative losses in the SW region, relative to chromospheric emission, remain the same even when the temperature of formation of the relavant lines changes from 10^5–10^4 K to $\lesssim 10^4$ K. Although we do not claim that the summed fluxes of lines between 1215 and 1950 Å (excluding O I) constitute a fundamental quantity, the relative constancy of this radiative loss ratio between stars with very different outer atmospheres encourages further analysis of the total radiative losses in all temperature regimes.

V. CONCLUSIONS

We have presented a survey of chromospheric and transition region line emission observable in the vacuum ultraviolet with the *IUE* satellite, making special efforts to indicate the quality of observed fluxes and the upper limits for non-detections. We find a wide variation of TR emission at a given position in the H-R diagram, which correlates well with chromospheric activity and with rotation. High temperature emission measures generally decrease with decreasing stellar gravity. The exact nature of this transition between "hot" and "cool" outer atmosphere is not well established due to the small sample size and to the sensitivity limits of the satellite, but there are reasons for preferring a more gradual change in the temperature structure than previously suggested. Where X-ray fluxes are available, the ratios of TR emission measures to X-ray emission measures are consistent with standard coronal theories. A first survey indicates that the outer atmospheres of many cool stars are very similar in structure to the solar atmosphere. The fluxes reported here provide a foundation for further investigations of the envelopes of late-type stars.

We gratefully acknowledge the assistance of the *IUE* observatory staff for assistance in the acquisition of these data. This work was supported by NASA grants NSG 5239, NSG 5370, and NAG 5-87.

REFERENCES

Athay, R. G. 1966, *Ap. J.*, **145**, 784.
Ayres, T. R., Linsky, J. L., Vaiana, G. S., Golub, L., and Rosner, R. 1981, *Ap. J.*, **250**, 293.
Ayres, T. R., Marstad, N. C., and Linsky, J. L. 1981, preprint.
Baliunas, S. L., and Butler, S. E. 1980, *Ap. J.* (*Letters*), **235**, L45.
Baliunas, S. L., Hartmann, L., and Dupree, A. K. 1980, in *The Universe at Ultraviolet Wavelengths, The First Two Years of IUE*, ed. R. D. Chapman, in press.
Barnes, T. G., and Evans, D. S. 1976, *M.N.R.A.S.*, **174**, 489.
Basri, G. S., and Linsky, J. L. 1979, *Ap. J.*, **220**, 619.
Beeckmans, F., and Penston, M. 1979, unpublished memo.
Boggess, A. *et al.* 1978, *Nature*, **275**, 361.
Bohlin, R., and Holm, A. 1980, *IUE NASA Newsletter*, No. 10, p. 37.
Bohlin, R. C., Holm, A. V., Savage, B. D., Snijders, M. A. J., and Sparks, W. M. 1980, *Astr. Ap.*, **85**, 1.
Bohlin, R. C., and Snijders, M. A. J. 1978, *IUE NASA Newsletter*, No. 2.
Bopp, B. W., and Espenak, F. 1977, *A.J.*, **82**, 916.
Brown, A., and Jordan, C. 1980, *M.N.R.A.S.*, in press.
Brown, A., Jordan, C., and Wilson, R. 1979, in *The First Year of IUE*, ed. A. J. Willis (London: University College London), p. 232.
Cassatella, A., Holm, A., Ponz, D., and Schiffer, F. H., III. 1980, *IUE NASA Newsletter*, No. 8.
Cassatella, A., Ponz, D., and Selvelli, P. L. 1981, *IUE NASA Newsletter, No. 14*, p. 170.
Catura, R. C., Acton, L. W., and Johnson, H. M. 1975, *Ap. J.* (*Letters*), **196**, L47.
de Loore, C. 1968, *Ap. Space Sci.*, **6**, 60.
Deutsch, A. J. 1956, *Ap. J.*, **123**, 210.
———. 1960, in *Stars and Stellar Systems*, Vol. **6**, *Stellar Atmospheres*, ed. J. L. Greenstein (Chicago: University of Chicago Press), p. 543.
Doschek, G. A., Feldman, U., Mariska, J. T., and Linsky, J. L. 1978, *Ap. J.* (*Letters*), **226**, L35.
Doyle, J., and Raymond, J. C. 1981, *Ap. J.*, in press.
Dupree, A. K. 1972, *Ap. J.*, **178**, 527.
———. 1975, *Ap. J.* (*Letters*), **200**, L27.
Dupree, A. K., Black, J. H., Davis, R. J., Hartmann, L., and Raymond, J. C. 1979, in *The First Year of IUE*, ed. A. J. Willis (London: University College London), p. 217.
Dupree, A. K., and Cruddance, R. 1981, in preparation.
Dupree, A. K., Goldberg, L., Noyes, R. W., Parkinson, W. H., Reeves, E. M., and Withbroe, G. L. 1973, *Ap. J.*, **183**, 321.
Dupree, A. K., and Hartmann, L. 1980, in *IAU Colloquium 51*, *Stellar Turbulence*, ed. D. F. Gray and J. L. Linsky (Berlin: Springer-Verlag), p. 279.
Giacconi, R. *et al.* 1979, *Ap. J.*, **230**, 540.
Haisch, B. M., and Linsky, J. L. 1976, *Ap. J.* (*Letters*), **205**, L39.
Hall, D. S. 1976, in *Multiple Periodic Variable Stars*, ed. W. S. Fitch (Dordrecht: Reidel), p. 287.

Hartmann, L., Davis, R., Dupree, A. K., Raymond, J., Schmidtke, P. C., and Wing, R. F. 1979, *Ap. J.* (*Letters*), **233**, L69.
Hartmann, L., Dupree, A. K., and Raymond, J. C. 1980, *Ap. J.* (*Letters*), **236**, L143.
———. 1981, *Ap. J.*, **246**, 193.
Hartmann, L., and MacGregor, K. B. 1980, *Ap. J.*, **242**, 260.
Harvel, C. A., Turnrose, B. E., and Bohlin, R. C. 1979, *IUE NASA Newsletter*, No. 5.
Holm, A. V. 1979, *IUE NASA Newsletter*, No. 7.
Holzer, T. E. 1980, SAO Special Report 389, p. 153.
Johnson, H. L., Mitchell, R. I., Iriate, B., and Wisniewski, W. F. 1966, *Comm. Lunar Planet. Lab*, **4**, 99.
Kraft, R. P. 1967, *Ap. J.*, **150**, 551.
Linsky, J. L., and Ayres, T. R. 1978, *Ap. J.*, **220**, 619.
Linsky, J. L. *et al.* 1978, *Nature*, **275**, 389.
Linsky, J. L., and Haisch, B. M. 1979, *Ap. J.* (*Letters*), **229**, L27.
Morgan, W. W., and Keenan, P. C. 1973, *Ann. Rev. Astr. Ap.*, **11**, 29.
Mullan, D. J. 1978, *Ap. J.*, **266**, 151.
Nussbaumer, H., and Schild, R. 1979, *Astr. Ap.*, **75**, L17.
Raymond, J. C., and Dupree, A. K. 1978, *Ap. J.*, **222**, 379.
Raymond, J. C., Noyes, R. W., and Stopa, M. 1979, *Solar Phys.*, **61**, 271.
Raymond, J. C., and Smith, B. W. 1977, *Ap. J. Suppl.*, **35**, 419.
Renzini, A., Cacciari, C., Ulmschneider, P., and Schmitz, F. 1977, *Astr. Ap.*, **61**, 39.
Rosner, R., Tucker, W. H., and Vaiana, G. S. 1978, *Ap. J.*, **220**, 643.
Skumanich, A. 1972, *Ap. J.*, **171**, 565.
Stein, R. F., and Leibacher, J. 1980, in *IAU Colloquium 51, Stellar Turbulence*, ed. D. F. Gray and J. L. Linsky (Berlin: Springer-Verlag), p. 225.
Stencel, R., and Ayres, T. 1980, preprint.
Stencel, R. E., Mullan, D. J., Linsky, J. L., Basri, G. S., and Worden, S. P. 1980, *Ap. J. Suppl.*, **44**, 383.
Stern, R., Underwood, J. H., Zolcinski, M.-C., and Antiochos, S. 1980, SAO Special Report 389, p. 127.
Topka, K., Fabricant, D., Harnden, F. R., Jr., Gorenstein, P., and Rosner, R. 1979, *Ap. J.*, **229**, 661.
Vaiana, G. S., and Rosner, R. 1978, *Ann. Rev. Astr. Ap.*, **16**, 393.
Vaiana, G. S. *et al.* 1981, *Ap. J.*, in press.
Vernazza, J. E., and Raymond, J. C. 1979, *Ap. J.* (*Letters*), **228**, L89.
Vitz, R. C., Weiser, H., Moos, H. W., Weinstein, A., and Warden, E. S. 1976, *Ap. J.* (*Letters*), **205**, L35.
Walter, F. M., Cash, W., Charles, P. A., and Bowyer, S. 1980, *Ap. J.*, **236**, 212.
Walter, J., Charles, P., and Bowyer, S. 1978, *A.J.*, **83**, 1539.
Weymann, R. 1962, *Ap. J.*, **136**, 844.
Wilson, O. C. 1966, *Science*, **151**, 1487.
Withbroe, G. L. 1976, presented at Annual Meeting, American Geophysical Union.
Withbroe, G. L., and Gurman, J. B. 1973, *Ap. J.*, **183**, 279.

A. K. Dupree, L. Hartmann, and J. Raymond: Harvard-Smithsonian Center for Astrophysics, 60 Garden Street, Cambridge, MA 02138